Optical Studies of Hydroxypropyl Methylcellulose Thin Films Exposed to UV/Ozone

Nabawia A Abdel-Zaher[1], Manal TH Moselhey[2], Osiris W Guirguis[3]

[1]Textile Metrology Lab, National Institute for Standards, Giza, Egypt
[2]Al-Safwa High Institute of Engineering, Cairo, Egypt
[3]Biophysics Department, Faculty of Science, Cairo University, Giza, Egypt

Abstract Thin films of hydroxypropyl methylcellulose (HPMC) are prepared by solution casting technique and exposed to UV/ozone for different exposure times. The effect of exposure on the optical properties such as: near infrared (NIR), transmittance spectra in the spectral region 250–2500 nm of the films are studied. The changes in the optical parameters including: The CIE tristimulus values, color parameters, absorption coefficient, absorption edge, band tail width, optical band gap, extinction coefficient and color strength as well as refractive index, dispersion parameters and optical dielectric constant are determined as a function of UV/ozone exposure times. The results indicate that, the NIR spectra showed variations in the intensity, area, band width, and the absorbance values of some bands. These variations mean that there are changes in the molecular configuration as well as the bond vibration and structure of HPMC as the exposure time increases. It is also noticed from the data that the variations in the values of band tail and optical band gap with increase the exposure time may be due to HPMC-induced structural change in the system. In addition, it is recognized that exposure with UV/ozone plays a role in microstructure and macrostructure change occurring in the polymer matrix.

Keywords HPMC – UV/ozone irradiation - NIR spectroscopy - Color parameters and optical dispersion properties

Introduction

Biomaterials are a very useful element in improving human health according to their applications includes diagnostics, therapeutic treatments and emerging regenerative medicine.

Polymers have a wide spectrum of physical, mechanical, and chemical properties. This wide spectrum supported the extensive research, development, and applications of polymeric biomaterials [1-2].

Hydroxypropyl methylcellulose (HPMC) also commonly known as hypromellose is a cellulose derivative. It belongs to the group of cellulose ether manufactured by chemical modification of native cellulose. HPMC is off-white to beige as a powder or granular form. HPMC can be soluble in hot water and in mixed organic solvents to form non-toxic solutions with excellent transparent film forming capabilities and resistant to oil and lipids [3-4]. According to the physical and chemical properties of HPMC, many applications in the food, cosmetic, and pharmaceutical industries are found. HPMC is a coating agent and film-former used as an inactive ingredient in the pharmaceutical industry [5]. Most novel capsule materials are based on water-soluble cellulose derivates such as methylcellulose and Hydroxypropyl methycellulose [5]. Also, due to its high viscosity, HPMC is used in ophthalmic preparations as artificial tears for dry eyes [6]. In addition, HPMC is a material classified as a Generally Recognized As Safe (GRAS), and is included in the Food and Drug Administration (FDA) Inactive Ingredients Guide, as well as licensed to be used in medicine and as a food additive in the UK and Europe [7].

UV-irradiation can modify the surface properties of biopolymer film. Exposure to ultraviolet radiation may cause surface and structural modifications polymeric films as results of photo-oxidation process [8-9]. Also, exposure of the film surface to ozone (O_3) gives rise to surface oxidization as a consequence of O_3 formation-decomposition combined reactions which is also carried out with UV irradiation. After ozone treatment, degradation phenomenon may arise. This phenomenon is an unwanted one and can be controlled by adjusting

the exposure time. Vig (1985) reported that UV/ozone cleaning procedure is an effective method a variety of contaminants from surfaces [10]. Also, Bolon and Kunz (1972) reported that UV light has the ability to depolymerize a variety of thin films photoresist polymers [11]. They also recognized that enhanced cleaning occurred in the presence of ozone when polymer surfaces are exposed the resulting decomposition products were carbon dioxide and water [11].

In the present work, the effect of UV/ozone exposure with different exposure times (1, 2, 3 and 4 h) is investigated by performing UV/VIS/NIR analysis on the band structure of HPMC thin films. Variations in the group coordination in the near-infrared region are detected. In addition, the variations in color parameters, refractive index and optical dispersion properties of the unexposed and exposed HPMC films are also examined.

Materials and Methods:
Sample preparation:
Hydroxypropyl methyl cellulose (HPMC; Pharmacoat 606) with MW 133.4 kg/mol is supplied from Shin Etsu Chemical Co., Japan. Solution-cast method is used to prepare thin transparent films of HPMC [12]. This method depends on the dissolution weighted amount of HPMC in double distilled water. Complete dissolution is obtained by using a magnetic stirrer for about 2 h at 50 ^{o}C. To form the films (0.01 cm thickness and 10 cm diameter), the solution was cast onto stainless steel Petri dishes and kept at room temperature ($\approx$ 25 ^{o}C) for 7 days until the water completely evaporated. After drying the prepared HPMC films are exposed to UV/ozone with different exposure times (1, 2, 3 and 4 h) at a distance 20 cm from a high intensity low pressure mercury lamp without outer envelope - LRF 02971, 220 Volt and 200 Watt, made in Poland and placed in a cubic box of dimensions 60 x 60 x 60 cm. The samples are measured at room temperature as slabs of dimensions 1 x 4 cm.

UV/VIS/NIR spectroscopic measurements:
The optical transmittance spectra for the prepared HPMC films before and after exposure to UV/ozone are recorded in the region from 250 to 2500 nm by using a Shimadzu UV/VIS/NIR Double Beam Spectrophotometer (Japan) with standard illuminant C (1174.83) model V-530, band width 2.0 nm with accuracy ±0.05% covers the range 200-2500 nm. From the obtained transmittance data, the tristimulus transmittance values (x_t , y_t and z_t) are calculated according to the CIE Colorimetric System and CIE 1931 2-degree Standard Observer [13-14]. The CIE three dimensional (L*, U* and V*), color constants (a* and b*), whiteness index (W), chroma (C*) and hue (H) are also performed [13-15]. The effect of exposure on the absorption coefficient, absorption edge, band tail, optical band gap, extinction coefficient and color strength of the prepared films have been determined. The transmittance values are also used for the determination of the refractive index, dispersion parameters and optical dielectric constant as functions of UV/ozone exposure times. The recorded data for each composite were an average of three measurements taken from three slabs from the same film.

Results and Discussions:
NIR spectral analysis:
Fig. 1 and Table 1 illustrate the NIR transmittance spectra and the assignments of the most important bands in the region from 900 to 2500 nm for unexposed and exposed HPMC films to UV/ozone for different times. As shown from the figure, there is an observable decrease in the transmittance value for the whole spectrum of the sample with increasing the exposure time up to 4 h. In addition, variations in the band positions and intensity of the bands are observed which means that there are changes in the molecular configuration as the exposure time increases [16-17]. Clear variations are observed in the band areas and band width of the exposed HPMC samples compared with the unexposed one which reflect the variation in the elastic modulus of the films.
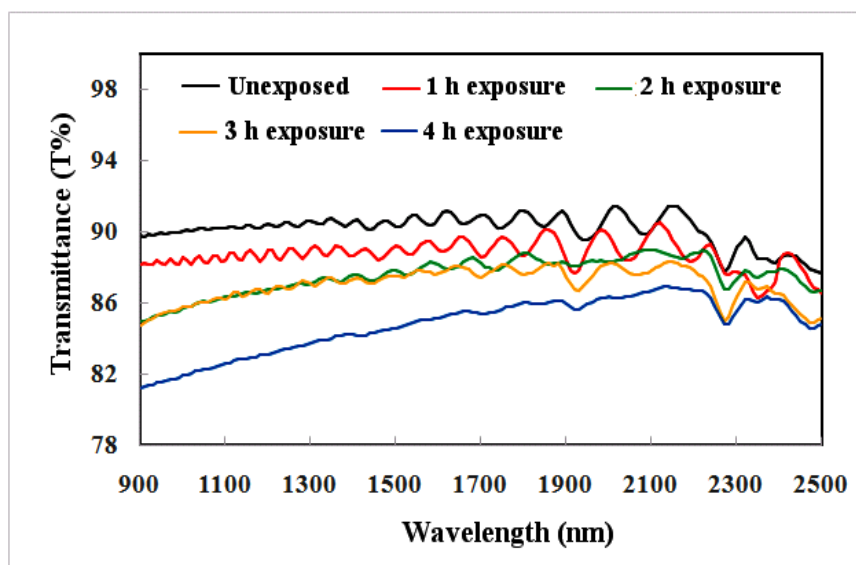
Figure 1: Variations in NIR transmittance spectra of unexposed and exposed HPMC films to UV/ozone with different times.

Table 1: Positions and assignments of the NIR transmittance bands of unexposed and exposed HPMC films to UV/ozone with different times.

Wavelength (nm)					Assignment	Chemical structure
UV/ozone exposure time (h)						
Unexposed	1	2	3	4		
2330	2330	2380	2370	2360	C-H deformation + second overtone cellulose	$HC=CHCH_2$
-	-	2210	2220	2220	C-H stretching + C=O stretching	$-CHO$
2160	2110	-	-	-	C-H stretching + C=O stretching	$-CHO$
1970	1985	1985	1985	1990	O-H stretching + O-H deformation	H_2O
1800	1860	1880	1870	1880	O-H stretching + 2(C-O) stretching	Cellulose
1782	1790	1785	1787	1782	C-H stretching first overtone	Cellulose
1700	1751	1775	1750	–	C-H stretching first overtone	CH_2
1641	1640	1636	1635	1650	C–H stretching	$HC=CH$
1376	1373	1370	1373	-	C-H stretching	2-C-H
1119	1133	1123	1121	-	C-H stretching	C-H
1053	1050	1053	1054	-	C-O stretching	Cellulose
945	945	946	946	-	O-H stretching + O-H deformation	H_2O

It is clear from Table 1 that, the band at 2330 nm for unexposed HPMC assigned to C-H deformation + second overtone cellulose shifted towards higher wavelengths by UV/ozone exposure to 2 h and then returns towards its original value with increasing the exposure times up to 4 h. The band at 2210 nm assigned to C-H stretching + C=O stretching appeared for 1 h exposure time and shifted towards higher wavelengths with increasing the exposure times up to 4 h. The band at 2160 assigned to C-H stretching + C=O stretching shifted towards lower wavelengths for 1 h exposure time and then disappeared with increasing the exposure times up to 4 h. The bands at 1970 nm assigned to O-H stretching + O-H deformation and 1880 nm assigned to O-H stretching + 2(C-O) stretching are shifted towards higher wavelengths by UV/ozone exposure up to 4 h. Nearly, no remarkable variation is detected for the bands at 1782 nm (assigned to C-H stretching first overtone) and at 1641 nm (assigned to C–H stretching) with exposure times up to 4 h. The band at 1770 nm assigned to C-H stretching first overtone shifted towards higher wavelengths by UV/ozone exposure up to 3 h and disappeared with

increasing the exposure time to 4 h. The bands at 1376, 1119 nm (assigned to C-H stretching), at 1053 nm (assigned to C-O stretching) and at 945 nm (assigned to O-H stretching + O-H deformation) indicate no remarkable variations in their positions with increasing the exposure times up to 3 h and then disappeared when the sample exposed to 4 h.

UV/VIS spectral analysis:

Optical absorption/transmission spectrum provides information about the band structure and the energy gap in amorphous and crystalline material. The study of the optical properties in the UV/VIS regions (250-700 nm) can help in understanding of the electronic structure and optical material [18-19]. From the data obtained of the transmittance values (Figure 1), the tristimulus transmittance values (x_t, y_t and z_t) of unexposed and exposed HPMC samples are calculated and plotted as a function of wavelength (400-700 nm) and shown in Figure 2a-c. It is observed from the figures that, the behaviors of y_t, x_t and z_t of the unexposed and exposed HPMC samples are similar and no change in their peak positions are detected. Furthermore, x_t y_t and z_t values decrease with increasing the exposure time up to 4 h. Tables 2 and 3 represent the values of x_r, y_r and z_r and their percentage changes (Δx_t, Δy_t and Δz_t), respectively, at their peak positions for unexposed and exposed HPMC samples.
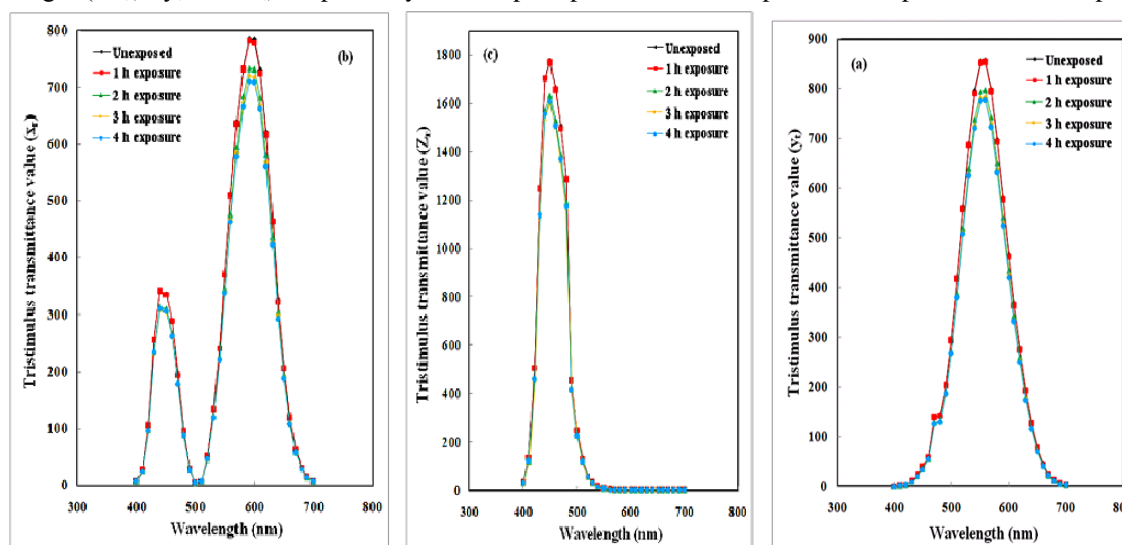

Figure 2: Variations in the tristimulus transmittance values: (a) x_t, (b) y_t and (c) Z_t as functions of wavelength for unexposed and exposed HPMC to UV/ozone with different times.

Table 2: Tristimulus transmittance values (x_r, y_r and z_r) for unexposed and exposed HPMC to UV/ozone with different times at their peak positions.

UV/ozone exposure time (h)	x_r		y_r	z_r
	λ = 445 nm	λ = 595 nm	λ = 555 nm	λ = 450 nm
Unexposed	345.257	787.010	858.230	1773.217
1	344.167	783.588	854.290	1767.232
2	316.899	733.349	798.931	1631.434
3	310.887	723.594	786.027	1600.271
4	313.619	710.709	777.755	1610.59

Table 3: Percentage changes in the maximum tristimulus transmittance values for unexposed and exposed HPMC to UV/ozone with different times.

UV/ozone exposure time (h)	$(\Delta x_t)\%$		$(\Delta x_t)\%$	$(\Delta z_t)\%$
	λ = 445 nm	λ = 595 nm	λ = 555 nm	λ = 450 nm
Unexposed	-	-	-	-
1	0.32	0.43	0.46	0.34
2	8.21	6.82	6.91	8.00
3	9.95	8.06	8.41	9.75
4	9.16	9.70	9.38	9.17

From the obtained data in Tables 2 and 3, the observed changes in the tristimulus transmittance values reflect the damaged sites and change in the molecular configuration which indicates to the formation of new color centers due to exposure to UV/ozone [17, 20].

Table 4 represents the variations of color parameters such as; CIE three dimensional (L*, U* and V*), color constants (a* and b*), whiteness index (W), chroma (C*) and hue (H) and their percentage changes calculated from the transmitance curves (Fig. 1) for unexposed and exposed HPMC samples.

Table 4 The results of color parameters and their percentage changes for unexposed and exposed HPMC to UV/ozone with different times.

Color parametersHPMC samples	Blank	1h	2h	3h	4h
L*	94.74	94.56	92.05	91.43	91.15
(ΔL*)%	–	-0.19	-2.84	-3.49	-3.79
U*	0.199	0.198	0.199	0.199	0.198
(ΔU*)%	-	-0.50	0.00	0.00	-0.50
V*	0.471	0.470	0.471	0.471	0.470
(ΔV*)%	-	-0.21	0.00	0.00	-0.21
a*	0.22	0.16	0.37	0.25	0.11
(Δa*)%	–	-27.27	68.18	13.64	-50.00
b*	0.81	0.72	1.38	1.45	0.64
(Δb*)%	–	-11.11	70.37	79.01	-20.99
W	83.30	83.30	74.40	72.60	75.80
ΔW%	–	0.00	-10.68	-12.85	-9.00
C*	0.84	0.74	1.43	1.47	0.65
(ΔC*)%	-	-11.90	70.24	-75.00	-22.62
H	74.55	77.84	75.13	80.11	80.25
(ΔH)%	-	3.97	0.39	7.04	7.23

From the table it is noticed that: The relative brightness (L*) shows decrease in their values with increasing the exposure times up to 4 h which means that HPMC becomes fader in color. No remarkable variations are detected for the CIE dimensional (U* and V*). The value of the color constant (a*) for exposure sample to 2 h is higher than the other unexposed and exposed values while the sample exposed to 4 h UV/ozone has the lowest value which indicates that, there is an increase in red component instead of green one after exposing to 2 h and an increase in the green component instead of the red one after exposing to 4 h UV/ozone. The values of the color constant (b*) increase with increasing the exposure time up to 3 h which indicates that there in an increase in yellow component instead of blue one and then decreases to less than the unexposed value with exposure time to 4 h. The whiteness index (W) values decrease with increase the exposure times up to 4 h. The observed variation in the chroma values (C*) is similar to the obtained changes in color constant (b*) while the hue values (H) increase with increasing the exposure time up to 4 h. The obtained results indicate that variations in color difference are occurred due to the exposure to UV/ozone of HPMC samples. This may be attributed to change in physical bonds and then changes in the molecular configuration of HPMC are produced as mentioned before [17, 20]. These variations in the molecular configuration may lead to formation of new dopant centers of the polymeric material. Therefore, the obtained data of the color parameters are of great importance for the improvement of the optical properties of the HPMC.

Figure 3 shows the transmittance spectra of unexposed and exposed HPMC samples in (a) the wavelength (range 250-700 nm) and (b) the photon energy (range 1.7-5.5 eV - UV/visible region). It is clear from the figure that drops in the transmittance values are detected with increasing the exposure times up to 4 h. These variations in transmittance values may be attributed to change in the molecular configuration which may be due to modification in molecular structure introduced as a result of the degradation process [17].
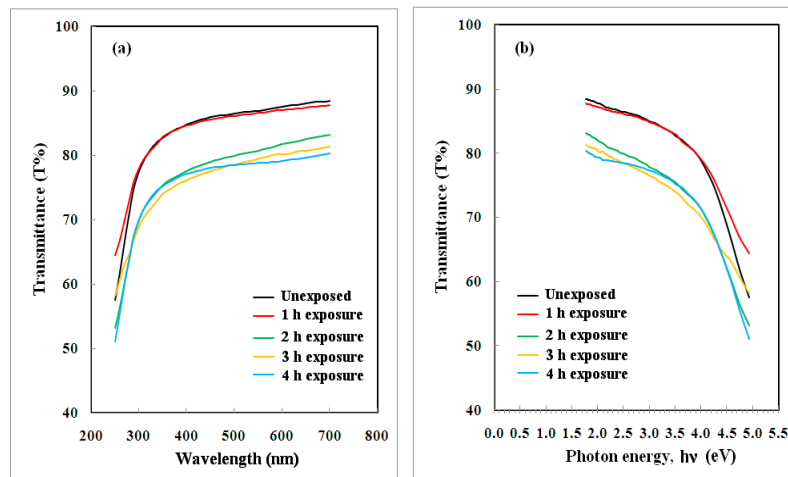
Figure 3: Dependence of transmittance spectra on wavelength (a) and photon energy, hv (b) for unexposed and exposed HPMC to UV/ozone with different times.

The absorption coefficient (α) of the unexposed and exposed HPMC films is calculated according to the relation [21-23]:

$$\alpha = \frac{1}{d} \ell n \frac{(1-R)^2}{T} \qquad (1)$$

d is the thickness of the sample in cm, T and R are the transmittance and reflectance values, respectively. Fig. 4a and b illustrates the relation between the absorption coefficients (α) as a function of wavelength and photon energy, respectively, for unexposed and exposed HPMC samples. It is clear from the figure that the absorption coefficient coefficient (α) values increase with increasing the exposure time up to 4 h through the whole wavelength and/or photon energy ranges. This increase may be attributed to the change of the molecular configuration which indicates to the formation of new color centers as well as may be due to modification in molecular structure introduced as a result of the degradation process, as previously mentioned and reported [17, 20].
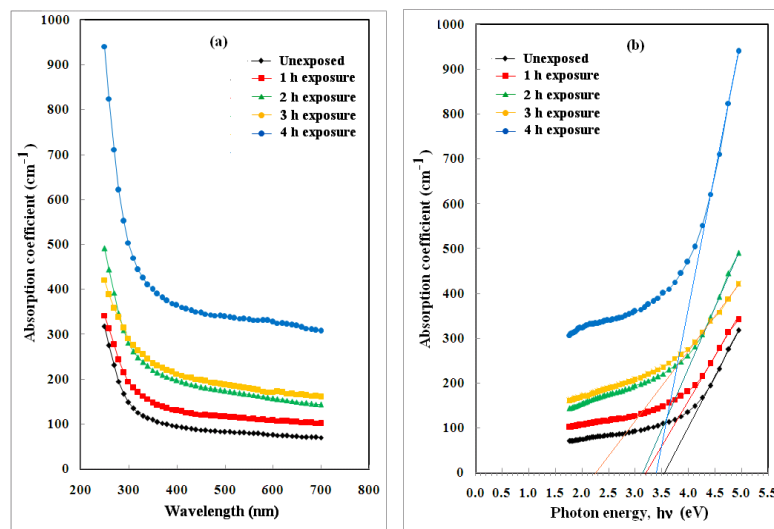

Figure 4: Plots of absorption coefficient against wavelength (a) and photon energy, hv (b) for unexposed and exposed HPMC to UV/ozone with different times.

The fundamental absorption edge is one of the most important features of the absorption spectra of crystalline and amorphous materials. It is clear from Fig. 4b that the absorption coefficient values (α) increases with increasing photon energy and a straight line relationship is deduced in the high α-region. The values of absorption edge (E_e) are calculated from the intercept of the extrapolation lines to zero absorption with photon energy axis and are listed in Table 5. It is clear that E_e values decrease with increasing exposure times up to 3 h

and then returns back to the value of the unexposed HPMC sample. This decrease in E_e indicates that exposure with UV/ozone leads to rupture of the bonds and formation of free radicals.

Table 5: Values of absorption edge (E_e), band tail energy (E_b), direct energy gap (E_d) and indirect energy gap (E_{ind}) for unexposed and exposed HPMC to UV/ozone with different times.

UV/ozone exposure time (h)	E_e (eV) UV-region	E_b (eV)		E_d (eV)		E_{ind} (eV) UV-region
		UV-region	Visible-region	UV-region	Visible-region	
Unexposed	3.533	0.984	5.181	4.210	2.166	2.883
1	3.214	1.312	5.587	4.066	2.108	2.376
2	3.133	1.344	4.878	4.016	2.079	2.386
3	2.254	2.364	4.975	3.882	2.022	1.530
4	3.398	1.224	9.091	4.156	1.906	2.676

For the amorphous nature of the polymeric materials, the energy which interpreted the width of the tail localized states in the normally forbidden band gap is given by applying Urbach relation as [21-23]:

$$\alpha = \alpha_o \exp\left[\frac{h\nu}{E_b}\right] \tag{2}$$

where α_o is a constant, ν is the frequency of radiation and E_b is the band tail energy value for each unexposed and exposed HPMC samples calculated from the inverse of the slopes of the straight lines represented by $\ell n\ \alpha$ against $h\nu$ (Fig. 5). From the figure, it is clear that, each curve can be divided into two straight lines for each sample, one of them in the UV region (3.2-5.5 eV) and the other in the visible region (1.7-3.1 eV). These straight lines suggested that the absorption follows the quadratic relation for inter-band transitions which verified Urbach rule (Mott and Davis; 1979). The values of band tail energy (E_b) for each region are calculated and listed in Table 5. The data indicate that, in the UV region, the values of E_b increase with increasing exposure times up to 3 h followed by a sharp decrease at 4 h exposure time. On the other hand, in the visible region, the values of E_b indicate irregular change with increases exposure times and maximum variation in the value of E_b is detected when the HPMC sample exposed to 4 h UV/ozone (i.e., increase by about 75%). From the data, the regular change (in UV region) and irregular change (in visible region) of E_b may arise from the variation in the total number available states which caused by UV/ozone according to the compromise between the degradation and crosslinking processes due to UV/ozone exposure [18-19]. Ion addition, the observed changes in E_b values may be due to the variation in the internal fields associated with structure disorder in the HPMC matrix [21].
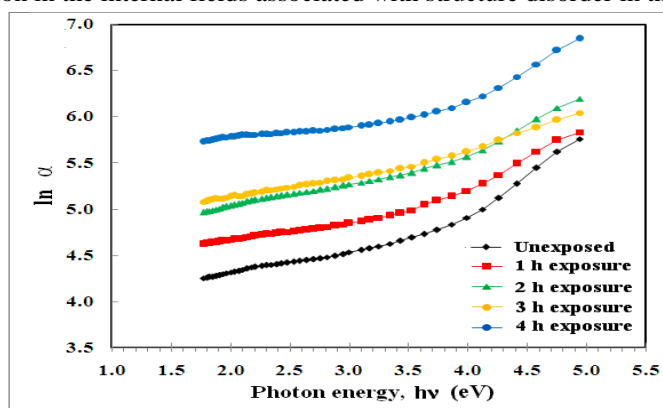

Figure 5: Dependence of $\ell n\ \alpha$ on $h\nu$ for unexposed and exposed HPMC samples to UV/ozone with different times.

The optical energy gap (E_g) of the unexposed and exposed HPMC thin films has been deduced from the absorption coefficient data as a function of photon energy. According to the accepted Tauc's model, the power part which obeys the Tauc [24] and Mott and Davis (1979) [21] is given from the relation as:

$$\alpha h\nu = B (h\nu - E_g)^n \tag{3}$$

where B is the slope of Tauc's edge called the band tail parameter in the range $10^5 - 10^6$ $(cm.eV)^{-1}$ and n is the electronic transition responsible type for absorption, being 1/2 or 2 for allowed direct and allowed indirect transitions, respectively. Fig. 6a shows the dependence of $(\alpha h\nu)^2$ on $h\nu$ in the range 1.7-5.5 eV for unexposed

and exposed HPMC samples. The inset of the figure shows the variation of $(\alpha h\nu)^2$ with hν in the visible region (1.7-3.1 eV). From the figure and the inset, the values of allowed direct energy gap (E_d) are calculated by extending the linear parts of the curves to zero absorption and are listed in Table 5. It is observed that, E_d values in both UV and visible regions decrease with increasing the exposure time up to 4 h. These decreases indicate that the values of E_d show the dependence on the composite and creation of localized states in the band gap as a result of exposure to UV/ozone for different times.
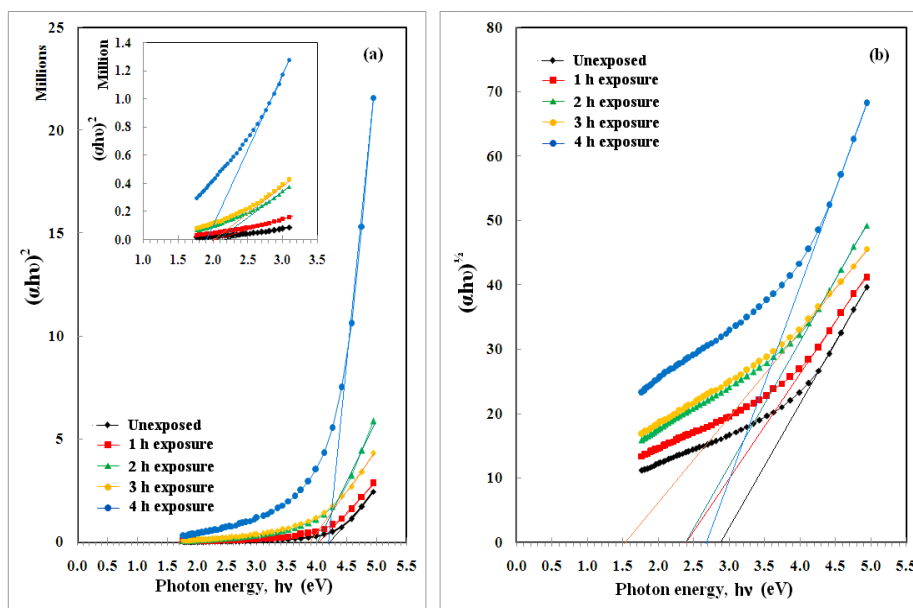

Figure 6: Plots of $(\alpha h\nu)^2$ (a) and $(\alpha h\nu)^{1/2}$ (b) versus photon energy, hν, for unexposed and exposed HPMC to UV/ozone with different times.

Figure 6b shows the change of $(\alpha h\nu)^{1/2}$ as a function of hν for unexposed and exposed HPMC samples. The allowed indirect energy gap (E_{ind}) values are also deduced by extrapolating the linear parts of the curves to zero absorption and are tabulated in Table 5. It is observed that the values of E_{ind} decrease with increasing exposure times up to 3 h and then returns back to the unexposed value with increasing the exposure time to 4 h. It may be presumed that the obtained decrease in the optical energy gap (direct and/or indirect allowed transitions) may be due to the change in molecular configuration induced by exposure with UV/ozone which leads to rupture of the bonds and formation of free radicals and then structural changes in the HPMC system are occurred [16-20].

Extinction coefficient and color strength determinations:

The extinction coefficient (K) presents the properties of the material to light. The extinction coefficient (k) is a parameter characterizes the photonic material and can be calculated by using the relation [22]:

$$K = \frac{\alpha\lambda}{4\pi} \tag{4}$$

Figure 7 shows the variation in the extinction coefficient (K) with wavelength of unexposed and exposed HPMC samples. It is clear that, the variation behaviors of K for all samples are similar through the whole wavelength range (250-700 nm) and their values are found to be small in the order 10^{-4}. This indicates that the prepared composites are considered to be insulating materials at room temperature [25]. In addition, the increase in the extinction coefficient values with increasing the exposure time up to 4 h shows that the fraction of light lost due to scattering.

The color strength (α/S) of the prepared HPMC films is determined by using Kubelka-Munk equation as [26]:

$$\frac{\alpha}{S} = \frac{(1-R)^2}{2R} \tag{5}$$

where α is the absorption coefficient, S is the scattering coefficient and R is the reflectance value. Figure 8 shows the dependence of the color strength (α/S) on wavelength (λ) for unexposed and exposed HPMC films to UV/ozone with different times. It is clear from the figure that the values of α/S increase with increasing wavelength and decrease markedly by increasing the exposure times up to 4 h. The observed decrease in α/S

values may be attributed the fact that the exposure HPMC samples give a fade color and structure disorder in the HPMC matrix which is in agreement with the data of the color parameters.
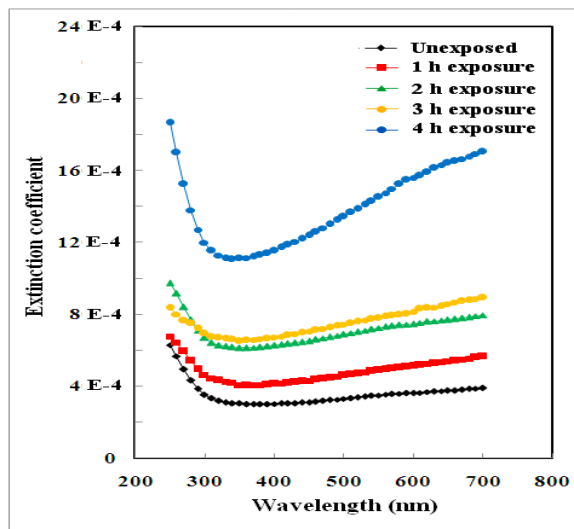

Figure 7: Dependence of the extinction coefficient, K, on wavelength, λ, for unexposed and exposed HPMC to UV/ozone with different times.
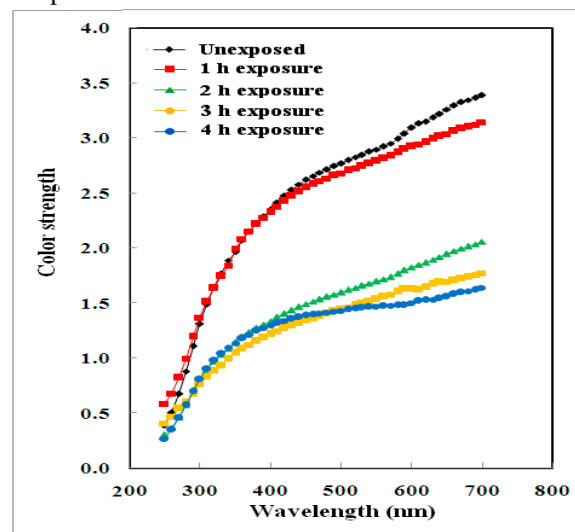
Figure 8: Dependence of the color strength, α/S, on wavelength, λ, for unexposed and exposed HPMC to UV/ozone with different times.

Optical dispersion parameters analysis:

From the reflectance (R) and extinction coefficient (K) data, the real part of the complex refractive index (n) of the prepared HPMC films is calculated according to the relation [27]:

$$n = \frac{1+R}{1-R} + \sqrt{\frac{4R}{(1-R)^2} - K^2} \qquad (6)$$

Figure 9 shows the refractive index distributions of unexposed and exposed HPMC films to UV/ozone with different times in the visible region. The figure reveals that the values of n of the exposed films increased markedly with increasing exposure time up to 4 h. Also, n values for each sample decrease with increasing the wavelength. The increased in the values of n may be caused when the incident light interacts with the exposed material, the refraction will be higher and hence the refractivity of the films will increase [28]. Such increases in n may allow these materials to be used as an anti-reflection coating for solar cells, or as high-refractive index lenses.
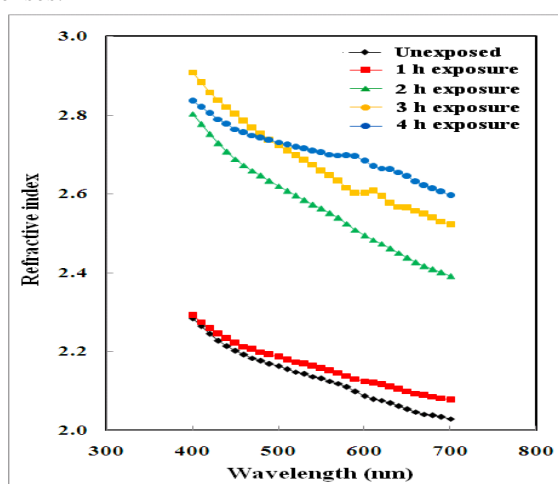

Figure 9: The variation of refractive index (n) as a function of wavelength (λ) for unexposed and exposed HPMC to UV/ozone with different times.
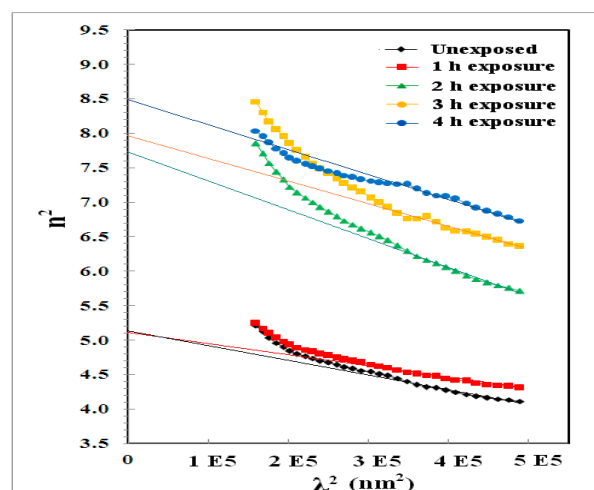
Figure 10: The dependence of n^2 on λ^2 for unexposed and exposed HPMC to UV/ozone with different times.

By plotting the variation of n^2 versus λ^2 and according to the dispersion relation [29]:

$$n^2 = \varepsilon_1 - \left[\frac{e^2 N}{\pi c^2 m^*} \right] \lambda^2 \tag{7}$$

The lattice dielectric constant (ε_1) and the ratio of carrier concentration to electron effective mass ($e^2N/\pi c^2 m^*$) can be calculated from the intercept and the slope of the straight line parts for unexposed and exposed HPMC samples (Fig. 10). Table 6 reveals that the values of the lattice dielectric constant (ε_1) increase with increasing the exposure time up to 4 h. In addition, irregular increase in the ($e^2N/\pi c^2 m^*$) ratio with increasing the exposure time is observed. This means that exposure to UV/ozone with different times increases the charge carrier concentration inside the HPMC matrix.

Table 6 Values of ε_1, ($e^2N/\pi c^2 m^*$), the energy parameter (E_p), the single oscillator energy (E_o), the long-wavelength refractive index (n_∞), λ_o is the average inter-band oscillator wavelength (λ_o) and the average oscillator strength (S_o) and their percentage changes for unexposed and exposed HPMC to UV/ozone with different times.

Dispersion parameters	HPMC/Exposure time (h)				
	Unexposed	1	2	**3**	**4**
ε_1	5.134	5.117	7.767	7.920	8.468
$\Delta\varepsilon_1$%	-	-0.33	51.29	54.27	64.94
($e^2N/\pi c^2 m^*$) x 10^{-6}	2.125	1.663	4.257	3.187	3.536
Δ($e^2N/\pi c^2 m^*$)%	-	-21.74	100.33	49.98	66.40
E_p (eV)	16.819	18.953	25.580	29.224	37.739
ΔE_p%	-	12.69	52.09	73.76	124.38
E_o (eV)	5.689	6.056	5.484	5.623	6.784
ΔE_o%	-	6.05	-3.60	-1.16	19.25
n_∞	2.002	2.040	2.367	2.452	2.582
Δn_∞%	-	1.90	18.23	22.48	28.97
λ_o (nm)	212	201	230	235	174
$\Delta\lambda_o$%	-	-5.19	8.49	10.85	-17.92
S_o (nm^{-2}) x 10^{-4}	0.669	0.783	0.870	0.932	1.868
ΔS_o%	-	17.04	30.04	39.31	179.22

Different dispersion parameters such as the energy parameter, E_p (a measure of the strength of inter-band optical transitions) and the single oscillator energy, E_o (the average excitation energy for electronic transitions) can be calculated from the change of n with λ on the basis of the model reported by Wemple and DiDomenico (1970) [30] as:

$$\frac{1}{n^2 - 1} = \frac{E_o}{E_p} - \frac{(h\nu)^2}{E_p E_o} \tag{8}$$

Figure 11a shows the variation of $(n^2-1)^{-1}$ as a function of $(h\nu)^2$ for unexposed and exposed HPMC to UV/ozone with different times. E_p and E_o values are obtained from the intercept and slope of the linear part from the figure and are tabulated in Table 6. It is noticed that the energy parameter (E_p) values markedly increase with increasing the exposure time up to 4 h.

In addition from the change of n with λ, the long-wavelength refractive index (n_∞), the average inter-band oscillator wavelength (λ_o) and the average oscillator strength (S_o) are also calculated by the dispersion equation as [27]:

$$\frac{1}{n^2 - 1} = \frac{1}{n_\infty^2 - 1} - \frac{\lambda_o^2}{n_\infty^2 - 1} \lambda^{-2} \tag{9}$$

Figure 11b shows the variation of $(n^2-1)^{-1}$ as a function of λ^{-2} for unexposed and exposed HPMC to UV/ozone with different times. The parameters n_∞, λ_o, and S_o [= $(n_\infty^2-1)/\lambda_o^2$] are obtained from the intercept and the slope of $(n^2 - 1)^{-1}$ versus λ^{-2} curves (Fig. 11b). The values of these parameters are given in Table 6. It is noticed from the data observed in the table that the dispersion parameters of HPMC are remarkably changed by exposure to UV/ozone with different exposure times.
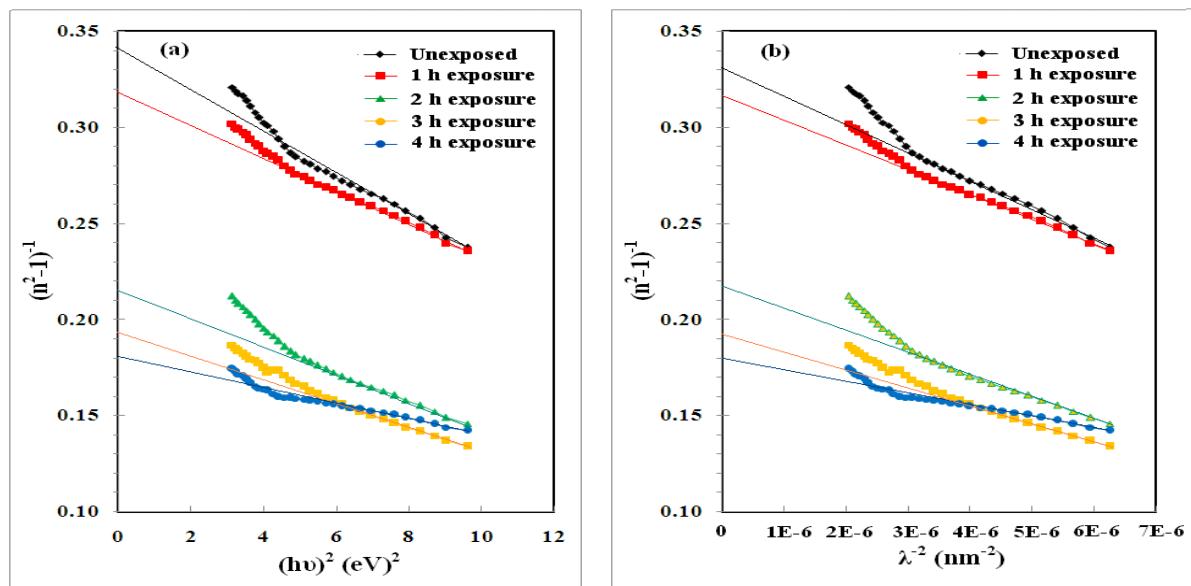
Figure 11: The variation of $(n^2-1)^{-1}$ as a function of $(h\upsilon)^2$ $(eV)^2$ (a) and λ^{-2} (b) for unexposed and exposed HPMC to UV/ozone with different times.

The real dielectric constant (ε_{real}) and imaginary dielectric constant ($\varepsilon_{imag.}$) can be calculated by using the following relations [31]:

$$\varepsilon_{real} = n^2(\lambda) - K^2(\lambda) \tag{10}$$
$$\varepsilon_{imag.} = 2\,n(\lambda)\,K(\lambda) \tag{11}$$

Figure 12a, b shows the variation in ε_{real} and $\varepsilon_{img.}$ as a function of photon energy ($h\upsilon$) for unexposed and exposed HPMC to UV/ozone with different times. It is clear from the figure that the values of ε_{real} and ε_{img} increase with increasing the exposure time up to 4 h. This variation in the frequency dependence of the optical dielectric constant due to exposure to UV/ozone gives information about the electronic excitations inside the materials.
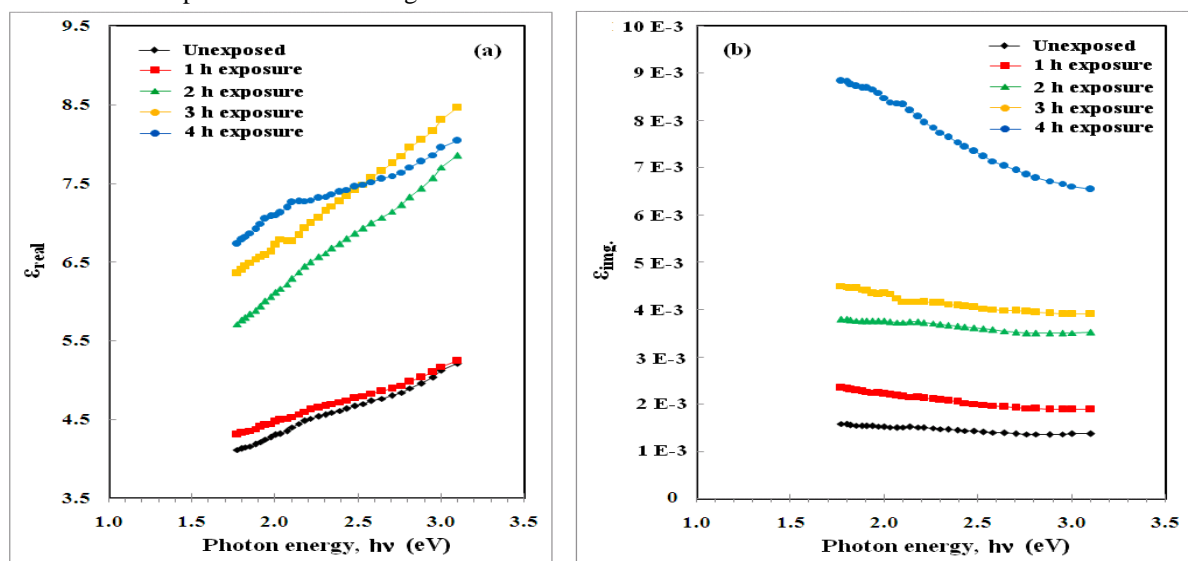

Figure 12. The variation in the real value, ε_{real} (a) and the imaginary value, $\varepsilon_{img.}$ (b) of the optical dielectric constant as functions of photon energy ($h\upsilon$) for unexposed and exposed HPMC to UV/ozone with different times.

Briefly, as previously reported [8,9] exposure to ultraviolet radiation may cause surface and structural modifications polymeric films as results of photo-oxidation process. Due to this process formation of hydroxyl and carbonyl groups in UV-irradiated polymers and biopolymers is accompanied. Also, exposure of the film surface to ozone (O_3) gives rise to surface oxidization as a consequence of O_3 formation-decomposition combined reactions which is also carried out with UV irradiation. Therefore, the technique under study can be employed as pre-treatment after which grafting of certain chemical entities can be accomplished.

Conclusion:

From the obtained data, it may conclude that, HPMC samples under investigation exhibit a radiation sensitization characteristic for each UV/ozone exposure time. In addition, the observed variations in the optical parameters determined from the transmittance spectra due to exposure to UV/ozone with different exposure times up to 4 h may be due to the changes occurred in the physical bonds and in the molecular configuration of HPMC. These variations may lead to formation of new color centers of the polymeric system. In addition, the results of the optical dispersion parameters are very important to improve the optical properties of HPMC. Therefore, the changes observed in the color parameters and optical dispersion parameters are mainly depended on the total quantity of UV/ozone radiation received by the material.

References:

[1]. Dumitriu, S. (1996). *Polymeric biomaterials*. Marcel Dekker Inc., New York.

[2]. He, W., & Benson R. (2013). *Handbook of biopolymers and biodegradable plastics*. A volume in Plastics Design Library, 87–107.

[3]. Hofenk-de Graaff, J. (1981). *Central research laboratory for objects of art and science*. Gabriel Metsustroat and 1071 EA: Amsterdam, The Netherlands.

[4]. Greener, I. K., & Fennema, O. (1989). Barrier properties and surface characteristics of edible, bilayer films. *Journal of Food Science*, 54(6):1393-1399.

[5]. Lee, C. – Y., Chen, G. – L., Sheu, M. – T., & Liu, C. – H. (2006). Drug release from hydroxypropyl cellulose and polyethylene oxide capsules: In vitro and in vivo assessment. *The Chinese Pharmaceutical Journal,* 58:57-65.

[6]. Herder, J., Adolfsson, Å., & Larsson, A. (2006). Initial studies of water granulation of eight grades of hypromellose (HPMC). *International Journal of Pharmaceutics*, 313(1-2):57-65.

[7]. Drozen, M. S., & Hill, D. W. (2006). *US food and drug administration-hydroxypropyl methylcellulose (HPMC) as being generally recognized as safe*. Retrived on December 15th.

[8]. Pocius, A. V. (2002). *Adhesion and adhesives technology: An introduction*. Hanser: Munich, Germany.

[9]. Sionkowska, A., Skopinska-Wisniewska, J., Planecka, A., & Kozlowska, J. (2010). The influence of UV irradiation on the properties of chitosan films containing keratin. *Polym. Deg. Stab*. 95:2486-2491.

[10]. Vig, J. R. (1985). UV/ozone cleaning of surfaces. *J. Vac. Sci. Technol. A* 3(3):1027-1034.

[11]. Bolon, D. A., & Kunz, C. O. (1972). Ultraviolet depolymerization of photoresist polymers. *Polym. Eng. Sci.* 12(2):109-111.

[12]. El-Zaher, N. A., & Osiris, W. G. (2005). Thermal and structural properties of poly(vinyl alcohol) doped with hydroxypropyl cellulose. *Journal of Applied Polymer Science,* 96:1914-1923.

[13]. *CIE Recommendation on Colorimetry* (1986). CIE Publ. No. 15.2. Central Bureau of the CIE, Vienna.

[14]. *CIE Recommendation on Uniform color spaces; Color Difference Equations, Psychometric Color Terms* (1971;1978). Suppl. No. 2 of CIE Publ. No. 15 (E-1.3.1), Paris.

[15]. Abd El-Kader, F. H., Gaafer, S. A., & Abd El-Kader, M. F. H. (2014). Characterization and optical studies of 90/10 (wt/wt%) PVA/b-chitin blend irradiated with γ-rays. *Spectrochimica Acta Part A: Molecular and Biomolecular Spectroscopy* 131:564–570

[16]. Lever, A. B. P. (1968). *Organic electronic spectroscopy*. Elsevier, Amsterdam, Netherland.

[17]. Miller, A. (1994). Handbook of optics. vol. 1, McGraw-Hill, New York, USA.

[18]. Abd El-Kader, F. H., Gafer, S. A., Basha, A. F., Bannan, S. I., & Basha, M. A. F. (2010). Thermal and optical properties of gelatin/poly(vinyl alcohol) blends. *Journal of Applied Polymer Science,* 118:413-420.

[19]. Chikwenze, R. A., & Nnabuchi, M. N. (2010). Effect of deposition medium on the optical and solid state properties of chemical bath deposited CdSe thin films. *Chalcogenide Letters*, 7:389-396.

[20]. Osiris W. G., & Moselhey. M. T. H., Optical study of poly(vinyl alcohol)/hydroxypropyl methylcellulose blends. *J. Mater. Sci.* 46:5775–5789.

[21]. Mott, N. F., & Davis, E. A. (1979). *Electronic processes in non-crystalline materials*. Oxford, Clarendon.

[22]. Tintu, R., Saurav, K., Sulakshna, K., Nampoori, V. P. N., Radhakrishnan, P., & Thomas, S. (2010). $Ge_{28}Se_{60}Sb_{12}$/PVA composite films for photonic applications. *J. Non-Oxide Glasses,* 2:167-174.

[23].Maradulin, A. A., Montroll, E. W., & G.H.Weiss, G. H. (1963). *Theory of lattice dynamics in the Harmonic Approximation*, Academic Press, New York, USA.

[24]. Wood, D. L., & Tauc, J. (1972). Weak absorption tails in amorphous semiconductors. *Phys. Rev. B,* 5:3144.

[25]. Pankove, J. L. (1975). *Optical process in semiconductors.* Devers Publication, New York, USA.

[26].Judd, D. B., & Wyszecki, G. (1975). *Color in business science and industry.* John Wiley & sons, Inc., 3rd Ed., New York.

[27]. El Sayed, A. M., Diab, H. M., & El-Mallawany, R. (2013). Controlling the dielectric and optical properties of PVA/PEG polymer blend via e-beam irradiation. *J. Polym. Res.* 20:1-10.

[28]. El Sayed, A. M., & Morsi, W. M. (2013). Dielectric relaxation and optical properties of polyvinyl chloride/lead monoxide nanocomposites. *Polym. Compos.* 34:2031–2039.

[29]. Chahal, R. P., Mahendia, S., Tomar, A. K., & Kumar, S. (2012). γ-Irradiated PVA/Ag nanocomposite films: Materials for optical applications. *Journal of Alloys and Compounds*, 538:212-219.

[30]. Wemple, S. H., & DiDomenico, Jr. M. (1970). Behavior of electronic dielectric constant in covalent and ionic materials. *Phys. Rev. B,* 3:1338.

[31]. Al-Ghamdi, A. A. (2006). Optical band gap and optical constants in amorphous $Se_{96-x}Te_4Ag_x$ thin films. *Vacuum*, 80:400–405.